Available online at www.sciencedirect.com

ScienceDirect

www.elsevier.com/locate/jes

JES JOURNAL OF ENVIRONMENTAL SCIENCES

www.jesc.ac.cn

Seasonal variation and sources of derivatized phenols in atmospheric fine particulate matter in North China Plain

Yang Yang [1], *Xingru Li* [1,*], *Rongrong Shen* [2], *Zirui Liu* [2], *Dongsheng Ji* [2], *Yuesi Wang* [2,*]

[1] *Department of Chemistry, Analytical and Testing Center, Capital Normal University, Beijing, 100048, China*
[2] *State Key Laboratory of Atmospheric Boundary Layer Physics and Atmospheric Chemistry, Institute of Atmospheric Physics, Chinese Academy of Sciences, Beijing, 100029, China*

ARTICLE INFO

Article history:
Received 23 July 2019
Received in revised form
23 October 2019
Accepted 25 October 2019
Available online 9 November 2019

Keywords:
Derivated phenols
Diurnal and seasonal variations
Correlation analysis
North China plain
$PM_{2.5}$

ABSTRACT

Qualitative and quantitative analyses of derivatized phenols in Beijing and in Xinglong were performed from 2016 to 2017 using gas chromatography-mass spectrometry. The results showed substantially more severe pollution in Beijing. Of the 14 compounds detected, the total average concentration was 100 ng/m^3 in Beijing, compared with 11.6 ng/m^3 in Xinglong. More specifically, concentration of nitro-aromatic compounds (NACs) (81.9 ng/m^3 in Beijing and 8.49 ng/m^3 in Xinglong) was the highest, followed by aromatic acids (14.6 ng/m^3 in Beijing and 2.42 ng/m^3 in Xinglong) and aromatic aldehydes (3.62 ng/m^3 in Beijing and 0.681 ng/m^3 in Xinglong). In terms of seasonal variation, the highest concentrations were found for 4-nitrocatechol in winter in Beijing (79.1 ± 63.9 ng/m^3) and 4-nitrophenol in winter in Xinglong (9.72 ± 8.94 ng/m^3). The analysis also revealed diurnal variations across different seasons. Most compounds presented higher concentrations at night in winter because of the decreased boundary layer height and increased heating intensity. While some presented higher levels during the day, which attributed to the photo-oxidation process for summer and more biomass burning activities for autumn. Higher concentrations appeared in winter and autumn than in spring and summer, which resulted from more coal combustions and adverse meteorological conditions. The significant correlations among NACs indicated similar sources of pollution. Higher correlations presented within each subgroup than those between the subgroups. Good correlations between levoglucosan and nitrophenols, nitrocatechols, nitrosalicylic acids, with correlation coefficients (r) of 0.66, 0.69 and 0.69, respectively, indicating an important role of biomass burning among primary sources.

* *Corresponding authors.*
E-mail addresses: lixr@cnu.edu.cn (X. Li), wys@dq.cern.ac.cn (Y. Wang).

https://doi.org/10.1016/j.jes.2019.10.015
1001-0742/

Introduction

Nitro-aromatic compounds (NACs) are classes of nitro derivatized phenols, including nitrophenols (NPs), nitrocatechols (NCs), nitrosalicylic acids (NSAs) and nitroguaiacols (NGAs). As important components of brown carbon, NACs can absorb the ultraviolet-visible light (Lin et al., 2017; Xie et al., 2017). They mainly originate from anthropogenic emissions, including automobile traffic (Morville et al., 2004; Tremp et al., 1993), herbicide and insecticide use (Harrison et al., 2005a), coal combustion (Lüttke et al., 1997) and biomass burning (Iinuma et al., 2010; Wang et al., 2017). Among these activities, biomass burning, traffic emission and coal combustion are regarded as the main sources, especially in urban areas (Morville et al., 2004; Claeys et al., 2012). NACs can also be formed in-situ by secondary reaction (Pereira et al., 2015; Yuan et al., 2016; Finewax et al., 2018), of which the most important route is the nitration of benzene and its derivatives, which can occur in both the aqueous and gas phases (Harrison et al., 2005a; 2005b). In the gas phase, the oxidation mechanism of phenol is initiated by OH radicals and then reacts with NO_x during the day (Olariu et al., 2002; Xu et al., 2013). At night, the reaction preferentially originates from NO_3 radicals (Bolzacchini et al., 2001). For instance, methyl-nitrocatechols can form from the oxidation of methoxyphenol in the presence of OH radicals and NO_x (Iinuma et al., 2010). The products of OH radical-initiated reactions of phenol and cresols (in the presence of NO_2) are nitrophenols (Atkinson et al., 2003). 2-Nitrophenol (2NP) and 4-nitrophenol (4NP) can be oxidized to 2,4-dinitrophenol (2,4-DNP) in the presence of NO_2 and OH radicals (Vione et al., 2009). In the aqueous phase, there are also many formation paths of NACs in the atmospheric. For instance, 2,4-DNP can be generated upon the nitration of 2NP or 4NP (Vione et al., 2005). The photochemical treatment of 4NP, 5-nitroguaiacol (5NGA) and 4-nitrocatechol (4NC) by direct photolysis and •OH oxidation has been investigated in a series of laboratory studies. The results indicated significant changes in the absorptive properties of the compounds (Zhao et al., 2015). Besides, NP can be removed through photolysis in the gas phase (Yuan et al., 2016) and react with OH radicals in the aqueous phase (Vione et al., 2009). Irradiated NPs can produce nitrite and nitrous acid (HONO) in bulk aqueous solutions and in viscous aqueous films (Barsotti et al., 2017). The photolysis of NP is an important source of HONO in the atmosphere (Vione et al., 2009).

As compared with NACs, there has been less analysis of aromatic aldehydes and acids, especially quantitative studies. These compounds are present with low concentrations in atmospheric particulate matter (Rousova et al., 2018). Studies have shown that aromatic aldehyde and acid compounds are the products of lignin degradation (Simoneit, 2002; Fabbri et al., 2009). For instance, vanillic (va-de), *p*-hydroxybenzoic acid (*p*-hbid), vanillic acid (va-id) and syringic acid (sy-id) come respectively from pine combustion, grass burning, softwood combustion and hardwood combustion (Simoneit, 2002; Oros et al., 2006). In addition, va-id and *p*-hbid have been used as biomass burning tracers in other research (Kawamura et al., 2012). *p*-hbid, va-id and sy-id are influenced by pH in the atmospheric aqueous phase and can form new chromophoric compounds through Fenton-like oxidation, and the new compounds are more stable than the three aromatic acids (Santos et al., 2015; Santos et al., 2016).

In order to have a more comprehensive understanding of the pollution of NACs, aromatic aldehydes and aromatic acids in $PM_{2.5}$ over the North China Plain (NCP), the present study provides effective data to discuss their concentrations as well as seasonal and diurnal variations. Furthermore, their sources are analyzed through correlation analysis with levoglucosan and pollutant gases to provide reference for formulating effective protection measures.

1. Experimental details

1.1. *Sample collection*

$PM_{2.5}$ samples were collected simultaneously at two typical sampling sites over the NCP, including one urban site, Beijing, and one rural site, Xinglong, from March 2016 to January 2017. The Xinglong site is located in the regional atmospheric background station of the Chinese Academy of Sciences (CAS) (40°23′N, 117°34.5′E), which is situated to the south of the main peak of the Yan Mountains in Hebei Province, China. According to the meteorological conditions, city size, industrial structure and ecotypes, these two sampling sites were selected to be representative of regional air pollution across North China. Medium-volume samplers (TH-150; Wuhan Tianhong Corporation, China) and quartz fiber filters ($\Phi = 90$ mm, Pall Life Sciences, Ann Arbor, MI, USA) were used for $PM_{2.5}$ sampling. Before and after sampling, the airflow rate was calibrated, and the flow rates of the samplers were set to 100 L/min. The quartz fiber filters were prebaked at 500°C for 4 h before sampling and were stored at −20°C after sampling until analysis. $PM_{2.5}$ samples were collected from 08:00 to 19:30 during the day and from 20:00 to 07:30 of the next day during the night. Field blank filters were sampled as normal samples but with a 5 min pump off. A total of 560 samples and 32 blanks were collected from the two sites, including 320 samples and 16 blanks from Beijing as well as 240 samples and 16 blanks from Xinglong.

1.2. *Sample analysis*

Detailed descriptions of the extraction, derivatization and gas chromatography-mass spectrometry (GC-MS) methods have been provided elsewhere (Li et al., 2017; Li et al., 2019). Briefly, one-quarter of each filter was put into a glass vessel and ultrasonically extracted three times for 20 min with 20 mL of a mixture of dichloromethane (DCM) (HPLC grade, >99.8%) and methanol (HPLC grade, > 99.8%) (1:2, V/V). After extraction, the combined solution was filtered through a glass fiber filter, concentrated to 1.5 mL at 35°C by a rotary evaporator (Buchi, Sweden), and blown down to dryness using a gentle nitrogen stream. After reaction with a mixture of 50 μL *N*,*O*-bis(trimethylsilyl)trifluoroacetamide (BSTFA) with 1% trimethylchlorosilane (TMCS) and 10 μL pyridine (5:1, V/V) at 70°C for 3 hr, the derivatives were diluted to 400 μL with *n*-hexane and hexamethylbenzene as the internal standard and analyzed by GC-MS (TQ8040, Shimadzu, Japan).

The GC column was an HP-5MS capillary column (30 m length, 0.25 mm diameter, 0.25 μm film thickness), and the carrier gas was high-purity helium with a velocity of 1.0 mL/min. A total of 1 μL of sample was injected into the GC in splitless mode. The GC temperature was programmed as follows: 50°C for 2 min, increase to 120°C at 15°C/min, isothermal hold for 5 min, increase to 290°C at 5°C/min, and isothermal hold for 10 min. The injector temperature was 250°C. The MS was operated in electron ionization (EI) mode at 70 eV, and the full scan ranged from *m*/z 50–550. Determinations were performed by using selected ion monitoring (SIM) mode, and the internal standard method was used for quantification. The mass spectra of the target compounds were compared with standard spectra from the National Institute of Standards and Technology (NIST, 2014). All the detected compounds were determined using the peak areas of the individual characteristic ions. In addition, the GC-MS response factors were estimated using authentic standards.

Detailed information on the investigated compounds, including their molecular formulas, structures, fragment ions and quantitative ions, retention time, method limits of quantification (LOQ), method precision (repeatability) and the recovery of sample extraction are presented in Table S1. Method LOQ was determined by whether the peak of target can be distinguished from the baseline since data processing needs to carry out the peak area integration of detected substances. LOQs range from 25 to 50 μg/L. Repeat injecting the same sample for five times, and the concentration repeatability was the method precision. It was ranging from 92.4% to 97.3%, indicating the method was precise. The recovery of sample extraction was higher than 80.2%, lower than 93.2%, showing an effective extraction of pollutants in $PM_{2.5}$.

All analytical procedures were monitored using strict quality assurance and control measures. Laboratory blanks, field blanks and solvent blanks were used to determine potential contamination. The purities of the DCM, *n*-hexane, and methanol solvents used exceeded 99.8%. Phthalate esters were the main contaminants found in the blanks. These trace contaminants did not interfere with the identification or quantification of the compounds of interest.

2. Results and discussion

2.1. Molecular composition

In this study, a total of 14 compounds were analyzed including nine NACs: three NPs (4NP, 3-methyl-4-nitrophenol (3M4NP), 2,4-DNP), two NCs (4NC, 4-methyl-5-nitrocatechol (4M5NC)), two NSAs (3-nitrosalicylic acid (3NSA), 5-nitrosalicylic acid (5NSA)), and two NGAs (4-nitroguaiacol (4NGA), 5NGA). Five lignin-resin products were also analysed, including two aromatic aldehydes (*p*-hydroxybenzaldehyde (*p*-hbde), va-de) and three aromatic acids (*p*-hbid, va-id, sy-id). The detailed structures can be found in Table S1.

On the whole, the average concentrations of analyzed compounds during the whole sampling period at the urban site, Beijing were higher than those found at the rural site, Xinglong. The average concentrations of the 14 compounds were respectively 100.3 ng/m^3 in Beijing and 11.6 ng/m^3 in Xinglong, indicating that air pollution at the urban site was more severe than that at the rural site (Fig. 1), which attributed to the more frequent human activities that increased the primary sources in city area. Studies have shown that biomass burning process can release NACs as well as aromatic aldehydes and acids to atmosphere (Oros et al., 2006; Wang et al., 2017). Coal combustion (Lüttke et al., 1997) and traffic emissions (Morville et al., 2004) also was important sources for NACs. Sampling site of Beijing was located in the urban center, surrounding numerous roads and residential areas. Severe traffic emissions in daily life was a prevalent phenomenon due to heavy traffic. Coal-fired power generation, biomass burning and other human activities were also numerous in Beijing. In contrary, sampling site of Xinglong was at the south of the main peak of the Yan Mountains, about 960 m above the sea level. Most of the surroundings were countryside. Small population led to less primary emissions than Beijing.

Of the three classes compounds, NACs were the most abundant species, with an average value of 81.9 and 8.49 ng/m^3 in Beijing and in Xinglong, followed by aromatic acids, with an average mass concentration of 14.6 and 2.42 ng/m^3 in Beijing and in Xinglong, and then aromatic aldehydes, with an average concentration of 3.62 and 0.681 ng/m^3 in Beijing and in Xinglong.

Among all the detected NACs, 4NP and 4NC were the most abundant at both sites, with average concentrations of 20.5 ± 20.1 and 22.2 ± 32.6 ng/m^3 in Beijing as well as 3.07 ± 2.91 and 0.768 ± 0.981 ng/m^3 in Xinglong, respectively. Similar results were appeared in other areas, such as Shanghai (Li et al., 2016), Beijing (Wang et al., 2019), Jinan, Wangdu (Wang et al., 2018) and Hong Kong (Chow et al., 2016) of China, indicating that 4NP and 4NC were the two most abundant substances of NACs in most areas in China. Concentrations of 5NSA and 3NSA were the second highest while 4NGA, 5NGA and 2,4-DNP were the lowest. In the three aromatic acids, *p*-hbid was the most abundant species, with an average concentration of 10.3 and 1.78 ng/m^3 in Beijing and in Xinglong, followed by va-id (2.48 ng/m3 in Beijing and 0.404 ng/m^3 in Xinglong) and sy-id (1.81 ng/m^3 in Beijing and 0.232 ng/m^3 in Xinglong).

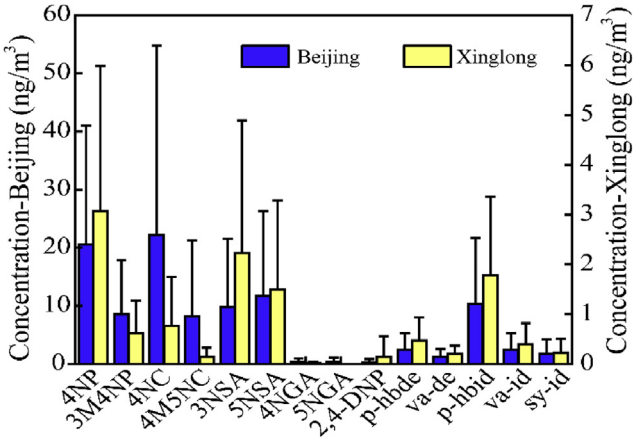

Fig. 1 – Average mass concentrations of the 14 compounds during the whole sampling period in Beijing and in Xinglong (the left y-axis was for Beijing data and the right for Xinglong data).

Concentration of p-hbde (2.46 ng/m^3 in Beijing and 0.471 ng/m^3 in Xinglong) was higher than that of va-de (1.17 ng/m^3 in Beijing and 0.210 ng/m^3 in Xinglong).

Detailed information on some of the analyzed compounds reported in previous studies is shown in Table 1. The concentrations of NACs in Beijing in this study were similar to some urban sites such as Shanghai (Li et al., 2016), but higher than those at some other urban sites such as Ljubljana (Kitanovski et al., 2012), Jinan (Wang et al., 2018), and Hong Kong (Chow et al., 2016). They were also higher than some rural sites, such as Yucheng and Wangdu, China (Wang et al., 2018) and Flanders, Belgium (Kahnt et al., 2013). Concentrations of aromatic acids in Beijing in this study were much higher than those in Nanjing, a city of China. While concentrations in Xinglong in this study were lower than Nanjing.

2.2. *Diurnal and seasonal variations*

In all four seasons in Beijing, most compounds presented higher concentrations at night than during the day, especially NPs in winter: for example, concentrations of 4NP and 3M4NP during the night were respectively 3.48 and 4.49 times higher than those during the day (Fig. 2). All compounds in winter showed a higher concentration at night, which was mainly affected by the decreased boundary layer height and increased coal combustion. The decreased boundary layer height allows pollutants to be accumulated, showing an increasing trend of concentration. Lower temperature at night leads to increased heating intensity, resulting in more coal combustion activities and more emissions of pollutants. During other seasons, some pollutant concentrations, such as 3NSA and *p*-hbid in spring; 4NP, 2,4-DNP, va-de and *p*-hbid in summer; and 4NP, 3M4NP, 4NC, 4M5NC and 2,4-DNP in autumn, were higher during the day than at night. The reason for higher concentrations of 4NP and 2,4-DNP in summer was relative to the secondary formation process. Major reaction pathway of 4NP and 2,4-DNP was photo-oxidation under the strong light intensity during daytime (Wang et al., 2019). Formation process of NACs (oxidation of toluene and benzene in the presence of NO_x) in summer was more important than the primary release, such as biomass burning (Wang et al., 2019). Concentration of all the NPs and NCs in autumn were higher during daytime, which attributed to the more biomass burning activities. Correlation analysis between NPs, NCs with levoglucosan of autumn is presented in Fig. 3. Significant correlations were found for NPs and NCs, with correlation coefficients (*r*) of 0.64 and 0.61, indicated that the primary source of biomass burning was important in autumn. More biomass burning activities during daytime lead to the higher concentrations.

In Xinglong, most of the analyzed compounds in spring, summer and autumn showed no significant diurnal variations because of their low atmospheric concentrations. In winter, most of them presented higher concentrations at night than during the day, to varying degrees: e.g., average 4NP concentrations of 13.38 ± 12.78 ng/m^3 were observed at night compared with 6.05 ± 5.09 ng/m^3 during the day. Significantly decreased boundary layer height and released from coal combustion at night in winter was the main reason for this phenomenon, which leads to the accumulation of pollutants.

Seasonal variations of the detected 14 compounds in Beijing and in Xinglong can be clearly seen in Table 2. The observed total concentrations as well as individual concentrations of the species were generally the highest in winter, followed by autumn and spring, and the lowest in summer. Increased human activities and adverse meteorological conditions resulted in the highest concentration of analyzed compounds in winter. The lower depth of the atmospheric mixed layer during winter was an important reason for the elevated concentrations. Moreover, indoor heating of residential areas and other buildings using coal energy aggravated the emission of pollutants in winter. Low temperatures also favored the partitioning of semi-volatile organic compounds, such as NPs, into the particle phase (Harrison et al., 2005a). For autumn, more biomass burning emissions in the surrounding areas led to the high concentrations. While in summer, higher atmospheric mixed layer was benefit to the diffusion of pollutants. Decreased human activities also reduced the primary emissions. Strong light intensity promoted the gas-phase loss pathways of some NACs (e.g. NP photolysis to HONO) (Vione et al., 2009). Those favorable conditions determined the light pollution in summer. Such seasonal patterns were similar to those founded at other sites, such as Hong Kong (Chow et al., 2016), Jinan (Wang et al., 2018), and Ljubljana, Slovenia (Kitanovski et al., 2012), where concentrations were higher in winter and autumn but lower in spring and summer.

2.3. *Correlations among nitroaromatic compounds, levoglucosan, and pollutant gases*

2.3.1. *Correlations among the detected nitroaromatic compounds*

Correlation analysis between two chemicals can be used to explore similarities in source or formation. To probe the relationships among the sources of NACs, correlation analysis of the Beijing and Xinglong data were conducted (Table 3). In Beijing, good correlations among the 9 NACs were found, with the correlation coefficients ranging from 0.42 to 0.91 (except for 5NSA and 5NGA), indicating similar sources of NACs, such as biomass burning, coal combustion and traffic exhaust. Interestingly, correlations within each subgroup, e.g. NPs (4NP and 3M4NP), NCs (4NC and 4M5NC), were stronger than those between subgroups, which suggested that the similarity of primary sources and secondary formation pathways was higher between the substances within each subgroup.

In Xinglong, good correlations also existed among NPs, NCs and NSAs, with correlation coefficients ranging from 0.54 to 0.96, showing a certain number of the same sources. Correlations within each subgroup were also higher than that between subgroups. NGAs and 2,4-DNP showed poor and even no correlations with the others, which may be related to the low concentrations that lead to few numbers of data of them.

2.3.2. *Correlation analysis with biomass burning tracers*

Biomass burning was a non-negligible source for NACs, aromatic aldehydes and aromatic acids (Iinuma et al., 2016). Study has shown that NACs were products of biomass by performing burning experiments with five common types

Table 1 – Mass concentration of aromatic compounds in comparison with previous studies.

Location	Time	Size	Compound	Concentration (ng/m^3)		Reference
				Range	Average ± SD	
Beijing	2016.3–2017.1	$PM_{2.5}$	NPs	n.d.-322	29.3 ± 30.4	This study
			NCs	n.d.-371	30.3 ± 45.7	
			NSAs	n.d.-367	21.5 ± 26.4	
			NGAs	n.d.-32.3	0.792 ± 1.22	
Xinglong	2016.3–2017.1	$PM_{2.5}$	NPs	n.d.-47.8	3.83 ± 3.98	
			NCs	n.d.-17.2	0.910 ± 1.17	
			NSAs	n.d.-34.8	3.73 ± 4.45	
			NGAs	n.d.-0.514	0.014 ± 0.033	
Shanghai	2013–2015	TSP	4NP	151–768	304	Li et al. (2016)
			MNPs	0.9–8	6.5	
			DNP	1–40	8	
			4NC	22–154	59	
			NGAs	12–175	70	
Jinan	2013.11–2014.1	$PM_{2.5}$	4NP	–	14.24	Wang et al. (2018)
			MNPs	–	12.34	
			4NC	–	8.54	
			MNCs	–	6.93	
			NSAs	–	6.36	
	2014.9	$PM_{2.5}$	4NP	–	2.47	
			MNPs	–	1.52	
			4NC	–	2.15	
			MNCs	–	1.18	
			NSAs	–	2.47	
Yucheng	2014.6	$PM_{2.5}$	4NP	–	1.32	
			MNPs	–	0.55	
			4NC	–	0.95	
			MNCs	–	0.39	
			NSAs	–	2.49	
Wangdu	2014.6	$PM_{2.5}$	4NP	–	1.48	
			MNPs	–	0.79	
			4NC	–	0.93	
			MNCs	–	0.77	
			NSAs	–	1.93	
HongKong	2010–2012	$PM_{2.5}$	4NP	n.d.-8.66	0.96 ± 1.24	Chow et al. (2016)
			MNPs	0.001–7.56	0.68 ± 0.96	
			4NC	0.004–24.9	2.31 ± 1.13	
			MNCs	0.004–25.8	1.73 ± 3.44	
Belgium	2010–2011	PM_{10}	4NP	–	0.65	Kahnt et al. (2013)
			4NC	–	1.91	
			MNCs	–	2.2	
Ljubljana	2010.8	PM_{10}	4NP	0.12–0.17	0.15	Kitanovski et al. (2012)
			DNP	<0.01	<0.01	
			4NC	0.16–0.35	0.24	
			MNCs	0.15–0.18	0.16	
			NGA	<0.11	<0.11	
			NSAs	0.2–0.36	0.27	
	2010.11–2011.1	PM_{10}	4NP	0.5–3.78	1.8	
			DNP	0.02–0.05	0.02	
			4NC	16.9–152	75	
			MNCs	17–134.7	69.2	
			NGA	0.4	<0.11-0.5	
			NSAs	0.3–7.3	2.7	
Roma	2003.3	PM_{10}	4NP	–	17.8 ± 5.6	Cecinato et al. (2005)
Beijing	2016.3–2017.1	$PM_{2.5}$	aromatic aldehydes	n.d.-42.7	3.62 ± 4.21	this study
			aromatic acids	n.d.-156	14.6 ± 16.5	
Xinglong	2016.3–2017.1	$PM_{2.5}$	aromatic aldehydes	n.d.-4.04	0.681 ± 0.635	
			aromatic acids	n.d.-21.1	2.42 ± 2.27	
Nanjing	2004.7	$PM_{2.5}$	va-id	0.23–2.6	0.86	Wang et al. (2005)
			sy-id	0.13–2.03	0.58	
	2005.1	$PM_{2.5}$	va-id	0.92–11	5.09	
			sy-id	0.48–8.83	3.33	

Full name of above compounds are nitrophenols for NPs, nitrocatechols for NCs, nitrosalicylic acids for NSAs, nitroguaiacols for NGAs, 4-nitrophenol for 4NP, methyl-nitrophenols for MNPs, 4-nitrocatechol for 4NC, dinitrophenol for DNP, vanillic acid for va-id and syringic acid for sy-id.

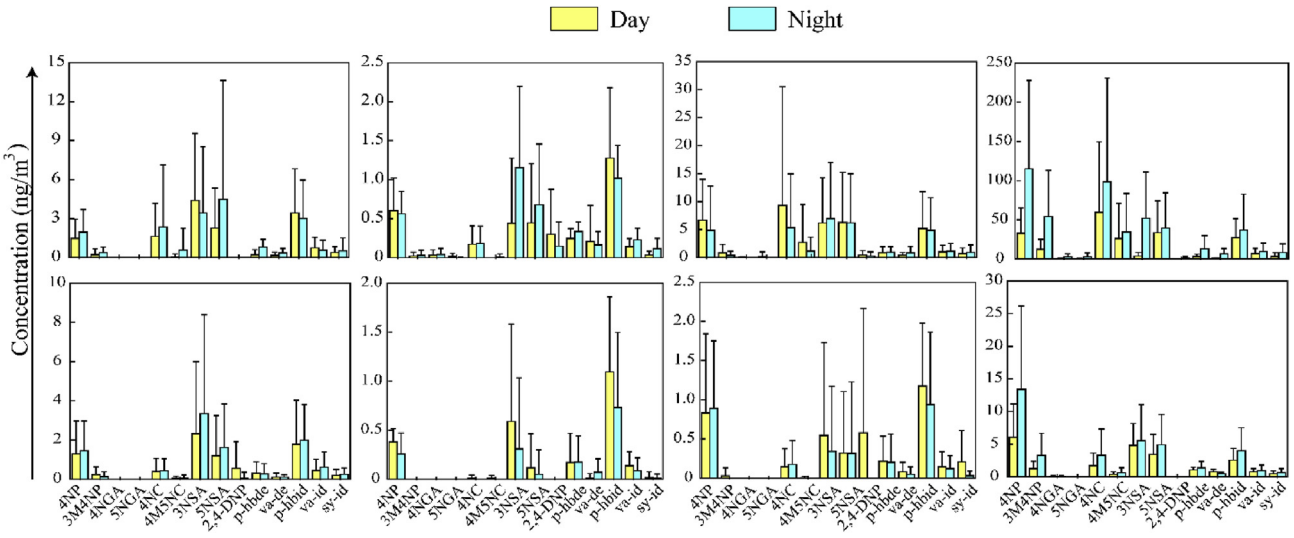

Fig. 2 – Diurnal variations of detected NACs in Beijing and Xinglong, respectively.

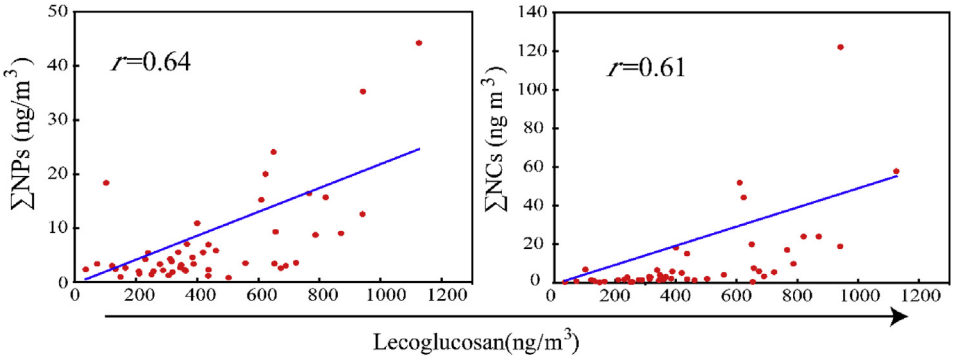

Fig. 3 – Correlation analysis between NPs, NCs and levoglucosan in Beijing autumn.

under different conditions (Wang et al., 2017). Levoglucosan, a thermal decomposition product of cellulose, was regarded as a tracer of biomass burning (Simoneit et al., 1999). To confirm the importance of biomass burning in the sources of NACs, the correlations of levoglucosan with NPs, NCs, and NSAs were conducted (Fig. 4). There were clear correlations between levoglucosan and NPs, NCs, and NSAs in Beijing, with correlation coefficients (*r*) of 0.66, 0.69, and 0.69. Variation patterns

Table 2 – Seasonal variations of detected organic compounds (ng/m³).

Compounds	Beijing				Xinglong			
	Spring	Summer	Autumn	Winter	Spring	Summer	Autumn	Winter
4NP	1.72 ± 1.60	0.58 ± 0.36	5.77 ± 7.63	74.05 ± 52.17	1.37 ± 1.60	0.32 ± 0.17	0.86 ± 0.93	9.72 ± 8.94
3M4NP	0.31 ± 0.43	0.02 ± 0.06	0.62 ± 1.10	33.13 ± 25.00	0.18 ± 0.32	n.d.	0.01 ± 0.05	2.28 ± 2.27
4NGA	n.d.	0.04 ± 0.00	0.01 ± 0.00	1.56 ± 1.42	0.00 ± 0.01	n.d.	n.d.	0.06 ± 0.12
5NGA	n.d.	0.01 ± 0.00	0.08 ± 0.00	1.48 ± 1.38	0.00 ± 0.00	n.d.	n.d.	n.d.
4NC	1.99 ± 3.66	0.18 ± 0.23	7.31 ± 5.40	79.10 ± 63.86	0.41 ± 0.65	n.d.	0.16 ± 0.27	2.50 ± 2.99
4M5NC	0.31 ± 0.95	0.01 ± 0.02	1.95 ± 4.62	30.22 ± 31.51	0.05 ± 0.13	n.d.	0.00 ± 0.01	0.51 ± 0.59
3NSA	3.92 ± 5.13	0.80 ± 0.94	6.59 ± 9.04	27.84 ± 5.38	2.84 ± 4.36	0.45 ± 0.86	0.45 ± 1.01	5.20 ± 4.42
5NSA	3.38 ± 6.11	0.56 ± 0.77	6.24 ± 8.86	36.50 ± 43.37	1.40 ± 2.14	0.08 ± 0.30	0.32 ± 0.85	4.18 ± 3.87
2,4-DNP	n.d.	0.22 ± 0.44	0.37 ± 0.76	0.57 ± 0.12	0.31 ± 0.83	n.d.	0.29 ± 0.79	n.d.
p-hbde	0.51 ± 0.50	0.29 ± 0.12	0.91 ± 1.05	8.12 ± 5.83	0.29 ± 0.55	0.17 ± 0.28	0.21 ± 0.34	1.22 ± 0.71
va-de	0.25 ± 0.31	0.19 ± 0.32	0.63 ± 0.83	3.59 ± 1.66	0.10 ± 0.17	0.04 ± 0.09	0.06 ± 0.11	0.64 ± 0.29
p-hbid	3.23 ± 3.18	1.15 ± 0.66	5.02 ± 6.21	31.96 ± 28.22	1.88 ± 2.03	0.91 ± 0.77	1.05 ± 0.86	3.28 ± 2.65
va-id	0.66 ± 0.79	0.19 ± 0.12	1.07 ± 1.30	7.99 ± 9.98	0.52 ± 0.68	0.11 ± 0.14	0.13 ± 0.18	0.85 ± 0.67
sy-id	0.46 ± 0.72	0.07 ± 0.09	0.81 ± 1.19	5.87 ± 7.15	0.22 ± 0.31	0.01 ± 0.05	0.12 ± 0.23	0.58 ± 0.51

n.d. Denoted not found. Full name of above compounds are 3-methyl-4-nitrophenol for 3M4NP, 4-nitroguaiacol for 4NGA, 5-nitroguaiacol for 5NGA, 4-methyl-5-nitrocatechol for 4M5NC, 3-nitrosalicylic acid for 3NSA, 5-nitrosalicylic acid for 5NSA, 2,4-dinitrophenol for 2,4-DNP, *p*-hydroxybenzaldehyde for *p*-hbde, vanillic for va-de and *p*-hydroxybenzoic acid for *p*-hbid.

Table 3 – Correlations among detected nitroaromatic compounds in Beijing and Xinglong, respectively.

	4NP		3M4NP		4NGA		5NGA		4NC		4M5NC		3NSA		5NSA		2,4-DNP	
	BJ	XL	BJ	XL	BJ	XL	BJ	XL	BJ	XL	BJ	XL	BJ	XL	BJ	XL	BJ	XL
4NP	1.00	1.00																
3M4NP	0.88	0.94	1.00	1.00														
4NGA	0.79	0.42	0.78	0.47	1.00	1.00												
5NGA	0.51	–	0.65	–	0.83	–	1.00	1.00										
4NC	0.77	0.86	0.57	0.80	0.63	0.30	0.43	–	1.00	1.00								
4M5NC	0.63	0.84	0.53	0.76	0.58	0.32	0.55	–	0.91	0.96	1.00	1.00						
3NSA	0.73	0.65	0.61	0.54	0.73	0.29	0.61	–	0.80	0.74	0.67	0.76	1.00	1.00				
5NSA	0.62	0.74	0.46	0.61	0.42	0.28	0.29	–	0.89	0.85	0.83	0.88	0.77	0.89	1.00	1.00		
2,4-DNP	0.52	–	0.62	–	0.72	–	0.73	–	0.52	–	0.60	–	0.67	–	0.49	–	1.00	–

Full name of BJ and XL are Beijing and Xinglong, respectively.

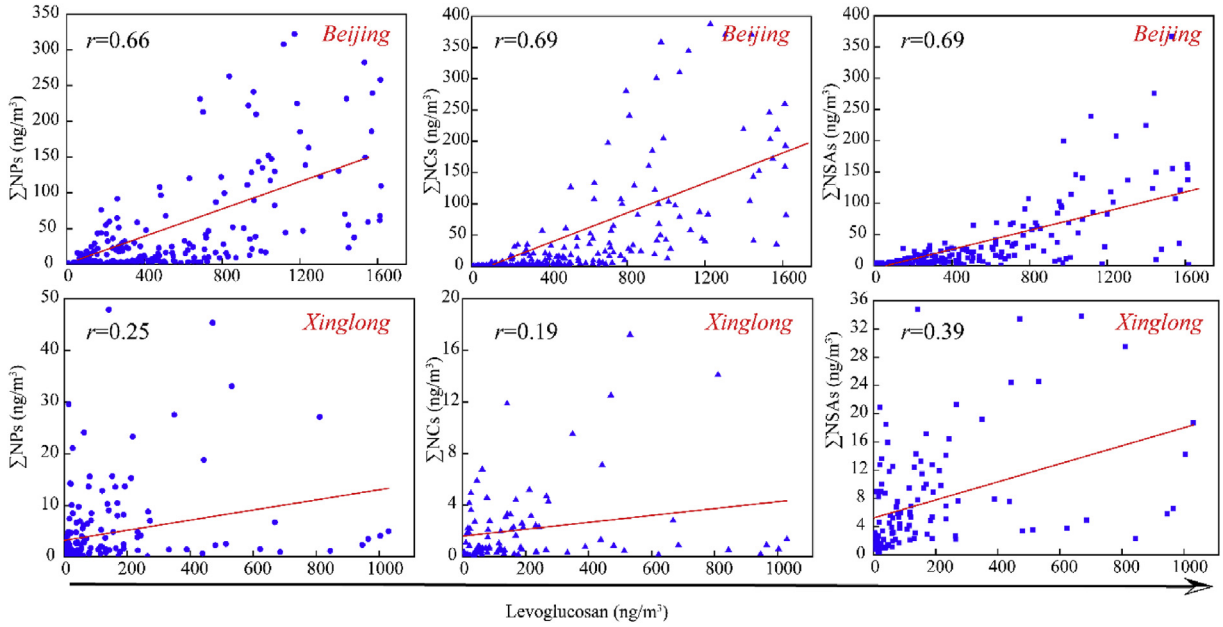

Fig. 4 – Correlations of levoglucosan with NPs, NCs, NSAs in Beijing and Xinglong.

of concentrations between levoglucosan and NPs, NCs, NSAs showed a high consistency in spring, autumn and winter (Fig. S1). While low consistency appeared in summer, which was related not only to lower levoglucosan concentrations resulting from lower intensity of biomass burning but also to the degradation of levoglucosan by reaction with OH radicals (Hoffmann et al., 2010). The high correlations and consistent variation patterns suggested that biomass burning was one important source of NPs, NCs, and NSAs in urban areas. Weak correlations were found between those compounds in Xinglong, with correlation coefficients (r) of 0.25, 0.19 and 0.39, respectively. The most important reason was the insufficient amount of data because of the lower concentrations of these compounds. At the same time, low concentrations brought some uncertainty to the detection, which also led to decreased of correlation.

Table 4 – Correlations of pollution gases with NPs, NCs, NSAs, aromatic aldehydes and aromatic acids in Bejing and Xinglong, respectively.

	Beijing					Xinglong				
	NPs	NCs	NSAs	aromatic aldehydes	aromatic acids	NPs	NCs	NSAs	aromatic aldehydes	aromatic acids
CO	0.61[b]	0.59[b]	0.56[b]	0.50[b]	0.64[b]	–	–	–	–	–
SO_2	0.40[b]	0.51[b]	0.46[b]	0.44[b]	0.57[b]	–	0.31[a]	–	–	0.23[b]
NO_2	0.53[b]	0.60[b]	0.57[b]	0.49[b]	0.65[b]	0.38[b]	–	–	–	0.30[b]

[a] Denoted that correlation is significant at 0.05 level (2-tailed), - denoted no correlation.; [b] Denoted that correlation is significant at 0.01 level (2-tailed)..

2.3.3. *Correlation analysis with pollutant gases*

Correlations of pollutant gases (CO, SO_2, NO_2) with NPs, NCs, NSAs, aromatic aldehydes and aromatic acids in Beijing and in Xinglong during the whole sampling period were analyzed. The correlation coefficients (*r*) were presented in Table 4. We can see that all the substances presented significant correlations with pollutant gases with *P* value less than 0.01 (two-tailed) in Beijing. Correlation coefficients (*r*) ranged from 0.40 to 0.65, indicating a good correlation. CO, SO_2 and NO_2 in the atmosphere were mainly from coal combustion, traffic exhaust, etc. The good correlations indicated an important role of these primary sources for NPs, NCs, NSAs, aromatic aldehydes and aromatic acids in Beijing. In Xinglong, correlations between pollutant gases with the five kinds of compounds were poor, which was similar to that of levoglucosan. The low concentrations resulted in a small amount of data and the uncertainty of detection, which was non-negligible cause for the poor correlations.

3. Conclusions

In order to evaluate the concentration, seasonal variation and sources of derivatized phenols in atmospheric fine particulate matter in NCP, China, $PM_{2.5}$ samples were collected simultaneously in Beijing and in Xinglong from March 2016 to January 2017 and analyzed using GC-MS. Influenced by more human activities, such as traffic emissions, biomass burning and coal combustion, higher concentrations of 14 analyzed compounds in Beijing were detected than in Xinglong, indicating a more severe pollution in the urban area. Among the 14 compounds, concentration of NACs was the highest, followed by aromatic acids and aromatic aldehydes both in Beijing and in Xinglong. Similar to other sites in China, 4NP and 4NC were the most polluting compounds of NACs.

Influenced by the lower depth of the atmospheric mixed layer and increased coal combustion activities, as well as the partitioning of semi-volatile organic compounds into the particle phase resulted from the low temperature, concentrations of 14 compounds appeared the highest in winter in Beijing and Xinglong. The decreased boundary layer height and increased heating intensity at night resulted in higher level pollution than during the daytime in the two sites in winter. Good correlations between NPs, NCs and levoglucosan in autumn in Beijing suggested biomass burning is the most important source for these pollutants. More biomass burning emissions in the surrounding areas was the cause for the high concentrations in autumn, especially during the daytime. In summer, higher atmospheric mixed layer and a relative reduction of human activities as well as the strong light intensity that promotes the gas-phase loss pathways of some NACs were all benefit for the light pollution, which determined the lowest concentrations among four seasons in the two sites. Photo-oxidation of 4NP and 2,4-DNP under strong light intensity led to higher concentrations in daytime than at night in summer.

Significant correlations found among NACs indicated similar sources for these pollutants, such as biomass burning, which can be proved by the good correlations with levoglucosan. Correlation analysis between pollutant gases with NPs, NCs, NSAs, aromatic aldehydes and aromatic acids also showed an important role of other primary sources, such as coal combustion, traffic exhaust, etc. Interestingly, correlations within each subgroup of NACs were stronger than those between different subgroups, suggesting that the similarity of primary sources and secondary formation pathways was higher between the substances within each subgroup. But due to low concentrations, analysis of both levoglucosan and pollutant gases in Xinglong presented poor correlations.

Acknowledgements

This work was supported by the National Key R&D Program of China (No: 2017YFC0210000) and the Ministry of Science and Technology of China (No: 2016YFC0202001).

Appendix A. Supplementary data

Supplementary data to this article can be found online at https://doi.org/10.1016/j.jes.2019.10.015.

REFERENCES

Atkinson, R., Arey, J., 2003. Atmospheric degradation of volatile organic compounds. Chem. Rev. 103, 4605–4638.

Barsotti, F., Bartels-Rausch, T., De Laurentiis, E., Ammann, M., Brigante, M., Mailhot, G., et al., 2017. Photochemical formation of nitrite and nitrous acid (HONO) upon irradiation of nitrophenols in aqueous solution and in viscous secondary organic aerosol proxy. Environ. Sci. Technol. 51, 7486–7495.

Bolzacchini, E., Bruschi, M., Hjorth, J., Meinardi, S., Orlandi, M., Rindone, B., et al., 2001. Gas-phase reaction of phenol with NO_3. Environ. Sci. Technol. 35, 1791–1797.

Cecinato, A., Di Palo, V., Pomata, D., Tomasi Sciano, M.C., Possanzini, M., 2005. Measurement of phase-distributed nitrophenols in Rome ambient air. Chemosphere 59, 679–683.

Chow, K.S., Huang, X.H.H., Yu, J.Z., 2016. Quantification of nitroaromatic compounds in atmospheric fine particulate matter in Hong Kong over 3 years: field measurement evidence for secondary formation derived from biomass burning emissions. Environ. Chem. 13, 665–673.

Claeys, M., Vermeylen, R., Yasmeen, F., Gómez-González, Y., Chi, X., Maenhaut, et al., 2012. Chemical characterisation of humic-like substances from urban, rural and tropical biomass burning environments using liquid chromatography with UV/vis photodiode array detection and electrospray ionisation mass spectrometry. Environ. Chem. 9, 273–284.

Fabbri, D., Torri, C., Simoneit, B.R.T., Marynowski, L., Rushdi, A.I., Fabiańska, M.J., 2009. Levoglucosan and other cellulose and lignin markers in emissions from burning of Miocene lignites. Atmos. Environ. 43, 2286–2295.

Finewax, Z., de Gouw, J.A., Ziemann, P.J., 2018. Identification and quantification of 4-nitrocatechol formed from OH and NO_3 radical-initiated reactions of catechol in air in the presence of NOx: implications for secondary organic aerosol formation from biomass burning. Environ. Sci. Technol. 52, 1981–1989.

Harrison, M.A.J., Barra, S., Borghesi, D., Vione, D., Arsene, C., Iulian Olariu, R., 2005a. Nitrated phenols in the atmosphere: a review. Atmos. Environ. 39, 231–248.

Harrison, M.A.J., Heal, M.R., Cape, J.N., 2005b. Evaluation of the pathways of tropospheric nitrophenol formation from benzene and phenol using a multiphase model. Atmos. Chem. Phys. 5, 1679–1695.
Hoffmann, D., Tilgner, A., Iinuma, Y., Herrmann, H., 2010. Atmospheric stability of levoglucosan: a detailed laboratory and modeling study. Environ. Sci. Technol. 44, 694–699.
Iinuma, Y., Böge, O., Gräfe, R., Herrmann, H., 2010. Methyl-nitrocatechols: atmospheric tracer compounds for biomass burning secondary organic aerosols. Environ. Sci. Technol. 44, 8453–8459.
Iinuma, Y., Keywood, M., Herrmann, H., 2016. Characterization of primary and secondary organic aerosols in Melbourne airshed: The influence of biogenic emissions, wood smoke and bushfires. Atmos. Environ. 130, 54–63.
Kahnt, A., Behrouzi, S., Vermeylen, R., Safi Shalamzari, M., Vercauteren, J., Roekens, E., et al., 2013. One-year study of nitro-organic compounds and their relation to wood burning in PM_{10} aerosol from a rural site in Belgium. Atmos. Environ. 81, 561–568.
Kawamura, K., Izawa, Y., Mochida, M., Shiraiwa, T., 2012. Ice core records of biomass burning tracers (levoglucosan and dehydroabietic, vanillic and p-hydroxybenzoic acids) and total organic carbon for past 300 years in the Kamchatka Peninsula, Northeast Asia. Geochim. Cosmochim. Acta 99, 317–329.
Kitanovski, Z., Grgic, I., Vermeylen, R., Claeys, M., Maenhaut, W., 2012. Liquid chromatography tandem mass spectrometry method for characterization of monoaromatic nitro-compounds in atmospheric particulate matter. J. Chromatogr. A 1268, 35–43.
Li, X., Jiang, L., Bai, Y., Yang, Y., Liu, S., Chen, X., et al., 2019. Wintertime aerosol chemistry in Beijing during haze period: Significant contribution from secondary formation and biomass burning emission. Atmos. Res. 218, 25–33.
Li, X., Jiang, L., Le, P.H., Yan, L., Xu, T., Yang, X., et al., 2016. Size distribution of particle-phase sugar and nitrophenol tracers during severe urban haze episodes in Shanghai. Atmos. Environ. 145, 115–127.
Li, X., Liu, Y., Li, D., Wang, G., Bai, Y., Diao, H., et al., 2017. Molecular composition of organic aerosol over an agricultural site in North China Plain: Contribution of biogenic sources to $PM_{2.5}$. Atmos. Environ. 164, 448–457.
Lin, P., Bluvshtein, N., Rudich, Y., Nizkorodov, S.A., Laskin, J., Laskin, A., 2017. Molecular chemistry of atmospheric brown carbon inferred from a nationwide biomass burning event. Environ. Sci. Technol. 51, 11561–11570.
Lüttke, J., Scheer, V., Levsen, K., Wünsch, G., Neil Cape, J., Hargreaves, K.J., et al., 1997. Occurrence and formation of nitrated phenols in and out of cloud. Atmos. Environ. 31, 2637–2648.
Morville, S., Scheyer, A., Mirabel, P., Millet, M., 2004. A multiresidue method for the analysis of phenols and nitrophenols in the atmosphere. J. Environ. Monit. 6, 963–966.
Olariu, R.I., Klotz, B., Barnes, I., Becker, K.H., Mocanu, R., 2002. FT-IR study of the ring-retaining products from the reaction of OH radicals with phenol, o-, m-, and p-cresol. Atmos. Environ. 36, 3685–3697.
Oros, D.R., Abas, M.R.b., Omar, N.Y.M.J., Rahman, N.A., Simoneit, B.R.T., 2006. Identification and emission factors of molecular tracers in organic aerosols from biomass burning: Part 3. Grasses. Appl. Geochem. 21, 919–940.
Pereira, K.L., Hamilton, J.F., Rickard, A.R., Bloss, W.J., Alam, M.S., Camredon, M., et al., 2015. Insights into the formation and evolution of individual compounds in the particulate phase during aromatic photo-oxidation. Environ. Sci. Technol. 49, 13168–13178.
Rousova, J., Chintapalli, M.R., Lindahl, A., Casey, J., Kubatova, A., 2018. Simultaneous determination of trace concentrations of aldehydes and carboxylic acids in particulate matter. J. Chromatogr. A 1544, 49–61.
Santos, G.T., Santos, P.S., Duarte, A.C., 2016. Vanillic and syringic acids from biomass burning: Behaviour during Fenton-like oxidation in atmospheric aqueous phase and in the absence of light. J. Hazard. Mater. 313, 201–208.
Santos, P.S.M., Duarte, A.C., 2015. Fenton-like oxidation of small aromatic acids from biomass burning in water and in the absence of light: implications for atmospheric chemistry. Chemosphere 119, 786–793.
Simoneit, B.R.T., 2002. Biomass burning — a review of organic tracers for smoke from incomplete combustion. Appl. Geochem. 17, 129–162.
Simoneit, B.R.T., Schauer, J.J., Nolte, C.G., Oros, D.R., Elias, V.O., Fraser, M.P., et al., 1999. Levoglucosan, a tracer for cellulose in biomass burning and atmospheric particles. Atmos. Environ. 33, 173–182.
Tremp, J., Mattrel, P., Fingler, S., Giger, W.J.W.A., Pollution, S., 1993. Phenols and nitrophenols as tropospheric pollutants: emissions from automobile exhausts and phase transfer in the atmosphere. Water Air Soil Pollut. 68, 113–123.
Vione, D., Maurino, V., Minero, Claudio, Pelizzetti, E., 2005. Aqueous atmospheric chemistry: formation of 2,4-dinitrophenol upon nitration of 2-nitrophenol and 4-nitrophenol in solution. Environ. Sci. Technol. 39, 7921–7931.
Vione, D., Maurino, V., Minero, C., Duncianu, M., Olariu, R.-I., Arsene, C., et al., 2009. Assessing the transformation kinetics of 2- and 4-nitrophenol in the atmospheric aqueous phase. Implications for the distribution of both nitroisomers in the atmosphere. Atmos. Environ. 43, 2321–2327.
Wang, G.H., Kimitaka, K., 2005. Molecular characteristics of urban organic aerosols from Nanjing: a case study of a mega-city in China. Environ. Sci. Technol. 39, 7430–7438.
Wang, L., Wang, X., Gu, R., Wang, H., Yao, L., Wen, L., et al., 2018. Observations of fine particulate nitrated phenols in four sites in northern China: concentrations, source apportionment, and secondary formation. Atmos. Chem. Phys. 18, 4349–4359.
Wang, X., Gu, R., Wang, L., Xu, W., Zhang, Y., Chen, B., et al., 2017. Emissions of fine particulate nitrated phenols from the burning of five common types of biomass. Environ. Pollut. 230, 405–412.
Wang, Y., Hu, M., Wang, Y., Zheng, J., Shang, D., Yang, Y., et al., 2019. The formation of nitro-aromatic compounds under high NOx and anthropogenic VOC conditions in urban Beijing, China. Atmos. Chem. Phys. 19, 7649–7665.
Xie, M., Chen, X., Hays, M.D., Lewandowski, M., Offenberg, J., Kleindienst, T.E., et al., 2017. Light absorption of secondary organic aerosol: composition and contribution of nitroaromatic compounds. Environ. Sci. Technol. 51, 11607–11616.
Xu, C., Wang, L., 2013. Atmospheric oxidation mechanism of phenol initiated by OH radical. J. Chromatogr. A 117, 2358–2364.
Yuan, B., Liggio, J., Wentzell, J., Li, S.M., Stark, H., Roberts, J.M., et al., 2016. Secondary formation of nitrated phenols: insights from observations during the Uintah Basin Winter Ozone Study (UBWOS) 2014. Atmos. Chem. Phys. 16, 2139–2153.
Zhao, R., Lee, A.K.Y., Huang, L., Li, X., Yang, F., Abbatt, J.P.D., 2015. Photochemical processing of aqueous atmospheric brown carbon. Atmos. Chem. Phys. 15, 6087–6100.